J. Electroanal. Chem., 138 (1982) 367–379
Elsevier Sequoia S.A., Lausanne – Printed in The Netherlands

THE ELECTROCHEMICAL BEHAVIOUR OF COBALT IN ALKALINE SOLUTIONS

PART II. THE POTENTIODYNAMIC RESPONSE OF $Co(OH)_2$ ELECTRODES

H. GOMEZ MEIER *, J.R. VILCHE and A.J. ARVÍA

Instituto de Investigaciones Fisicoquímicas Teóricas y Aplicadas (INIFTA), División Electroquímica. Sucursal 4—Casilla de Correo 16. (1900) La Plata (Argentina)

(Received 4th January 1982; in revised from 15th March 1982)

ABSTRACT

The potentiodynamic behaviour of $Co(OH)_2$ hydroxide electrodes is studied in the potential range related to the appearance of Co(III) and Co(IV) species. The corresponding electrochemical reactions involve relatively fast proton transfer processes occurring at potentials close to those predicted from thermodynamics. Sandwich-type structures of the electrode/film/solution interface are assumed in the interpretation of the processes. They probably include configurational changes of reactants and products participating in the various electrochemical reactions.

INTRODUCTION

The anodic formation of cobalt oxides has been studied by several authors since the works by Grube [1,2]. The electrochemical behaviour of cobalt has been investigated by potentiostatic and galvanostatic techniques [3–5] and voltammetry [6–9], using different electrolytes such as alkaline aqueous solutions [10–13], neutral solution containing KH_2PO_4(+NaOH) [14], borate solutions [14–19] and bicarbonate and borate solutions [20,21]. The different types of films produced at different potentials were studied by ellipsometry [18,19,22] and Mössbauer spectroscopy [23–26]. The equilibrium properties of the possible stoichiometric and non-stoichiometric film-forming species were also evaluated, including phase transition characteristics [27–36]. The electrocatalytic properties of Co(III) oxyhydroxide species, thermally prepared and reflected through the activity of the oxygen evolution reaction, were also considered in some detail [37–41].

The electrochemical reaction related to cobaltous hydroxide appears very complex and the interpretation advanced by different authors present some coincidences as well as clear discrepancies. There is agreement on the participation in those reactions

* Present address: Instituto de Química, Universidad Católica de Valparaíso, Chile.

0022-0728/82/0000–0000/$02.75

of oxides and hydroxides of various types. This has been concluded both from electrochemical as well as optical and structural studies of the anodically formed film. There is also evidence of the occurrence of various sandwich-type structures in the different potential regions. In this sense the work of Sato and co-workers [15–19] is relevant, as well as the conclusions derived from Mössbauer spectroscopy [23–26] made in situ.

The aim of the present work is to study the potentiodynamic response of cobaltous hydroxide electrodes in alkaline solutions in order to establish the actual degree of complexity of the electrochemical reaction and to develop a possible mechanistic understanding of that electrode.

EXPERIMENTAL

The experimental set-up was the same as previously described [42]. "Specpure" cobalt (Johnson Matthey Chem.) in the form of either fixed wires (0.5 mm diameter, 0.25 cm^2) or rotating discs (0.070 cm^2), and precipitated (colloid) cobalt hydroxide on vitreous carbon (Union Carbide, low density) discs (0.071 cm^2) substrates, supported with PTFE holders were used as working electrodes. The counter electrode was a large-area Pt sheet previously cleaned with the usual procedures.

Vitreous carbon was first polished with the finest grade emery paste, cleaned by immersion either in boiling dilute HCl or in a 1:1 $H_2SO_4 + HNO_3$ mixture, and finally rinsed in thrice-distilled water. The preparation of the vitreous carbon/$Co(OH)_2$ (colloid) working electrodes was carefully adjusted to obtain reproducible and comparable results. The $Co(OH)_2$ precipitation on the vitreous carbon substrate was made at room temperature from alternative immersions, first in a 0.01 *M* KOH + 0.33 *M* K_2SO_4 solution and then in a 5 m*M* $CoSO_4$ solution. The immersion time in both solutions was fixed at 10 s, and the number of alternative immersions in each solution covered was from 2 up to 30. The electrochemical measurements with the vitreous carbon/colloidal $Co(OH)_2$ electrode were performed in 0.01 *M* KOH + 0.33 *M* K_2SO_4 electrolytic solutions. For the "Specpure" cobalt working electrodes the following electrolytic solutions were employed: 1 *M* KOH (solution A); 0.1 *M* KOH (solution B); 0.1 *M* KOH + 0.3 *M* K_2SO_4 (solution C); 0.01 *M* KOH + 0.33 *M* K_2SO_4 (solution D); 2.5 *M* KOH (solution E). They were prepared from thrice-distilled water and analytical grade (p.a. Merck) reagents.

Potentials were measured vs. a Hg/HgO references electrode prepared by using the same KOH solution as employed in the experiments (Pt, H_2/KOH/HgO/Hg, $E^\circ = 0.926$ V). The correction for the liquid junction potential was taken into account, as previously described [42]. Experiments were made under N_2 gas saturation at 25°C using single (STPS), repetitive (RTPS) and triangularly modulated (TMTPS) triangular potential sweeps.

RESULTS

Cobalt/alkaline solution system

The E/I potentiodynamic profiles run in the -1.25–0.6 V range (Fig. 1) depend remarkably on the number of triangular potential sweeps. The first positive-potential-going scan exhibits the electroformation of Co(II) species in the -1.0–0 V range [42] and at more positive potentials a complex display of anodic peaks. The successive potential cycling produces a decrease in the current associated with the Co(II) electrochemical process, a change in distribution of the anodic current peaks related to oxidation states of Co greater than that of Co(II) and, simultaneously, the enhancement of the electroreduction current related to the latter species. Initially the anodic charge is much greater than the cathodic charge, but during the RTPS both charges approach the same value. The stabilized E/I profile which is attained after about 20–60 min shows two well-defined anodic current peaks, one at 0.1 V, another at 0.3 V and, probably, a third one beyond 0.5 V.

The distribution of current peaks becomes clearer when the cathodic switching potential is more positive than the potential for electroreducing the Co(II) species (Fig. 2). Under these circumstances the stabilized E/I profile involves equal anodic

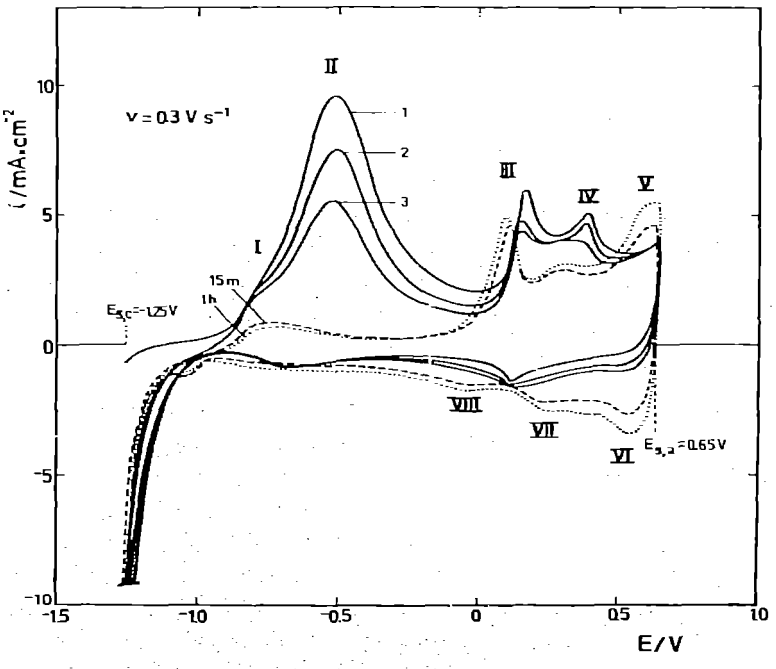

Fig. 1. Potentiodynamic E/I displays run with RTPS from -1.25 to 0.65 V at 0.3 V s^{-1}. The E/I curves for the first, second and third sweeps, together with those recorded after 15 min and 60 min potential cycling, are shown. Solution A.

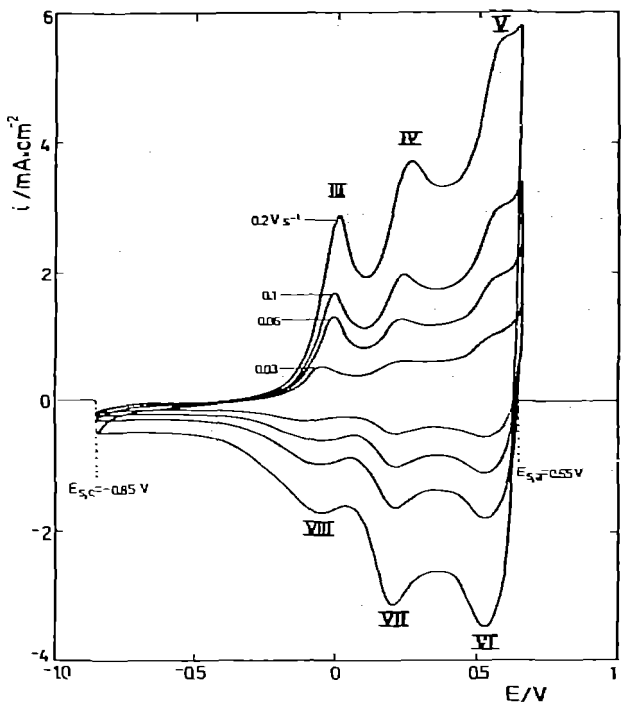

Fig. 2. Stabilized potentiodynamic E/I displays obtained with RTPS between −0.85 and 0.65 V at different scan rates. Solution A.

and cathodic charges and it exhibits three nearly reversible redox couples in the −0.1–0.6 V range. The height of each current peak depends linearly on the potential sweep rate (Fig. 3). The conjugated anodic and cathodic current peaks, as well as the electrochemical behaviour of each independent redox couple, can be determined by running TPS while gradually changing the anodic switching potential (Fig. 4). The kinetics of the redox couples appearing at the positive potential side are apparently faster than that of the first one. The appearance of the three redox couples requires that the Co(II) species remains on the electrode. This is achieved by properly selecting the value of the cathodic switching potential. These results suggest that the interphase acquires a sandwich-type structure where its outer side is related to the three redox reactions involving oxidation states of Co higher than that of Co(II). When the cathodic switching potential is equal to 0 V, the RTPS shows only the redox couples appearing in the 0–0.65 V range (Fig. 5). Therefore, by properly adjusting the cathodic switching potential, the stabilized E/I profile shows the contributions of the various redox processes well separated. This indicates that the three electrochemical processes are consecutive processes. The characteristics of the Co/alkaline solution interphase referred to above are independent of the alkaline solution concentration ($0.01\ M \leq c_{KOH} \leq 2.5\ M$).

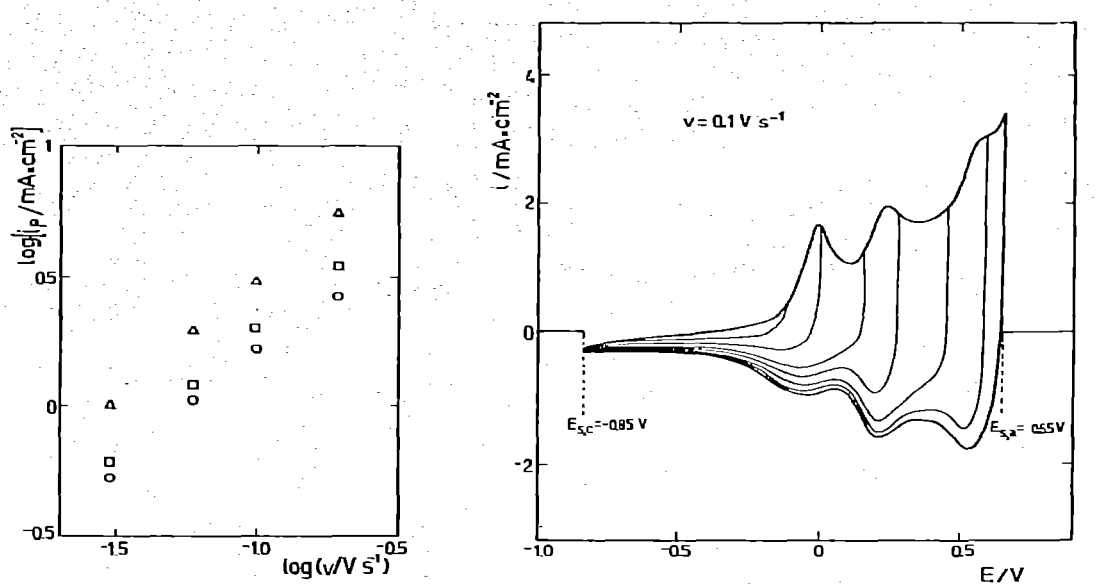

Fig. 3. Dependence of $i_{p,III}$ (○), $i_{p,IV}$ (□) and $i_{p,V}$ (△) on v from RTPS. Solution A.

Fig. 4. Influence of the anodic switching potential on the potentiodynamic E/I contour at 0.1 V s^{-1}. Solution A.

It is interesting to observe that although the three redox couples which appear at high positive potentials behave as independent reactions, they have a remarkable influence on the electroreduction processes taking place between −0.9 and −1.2 V

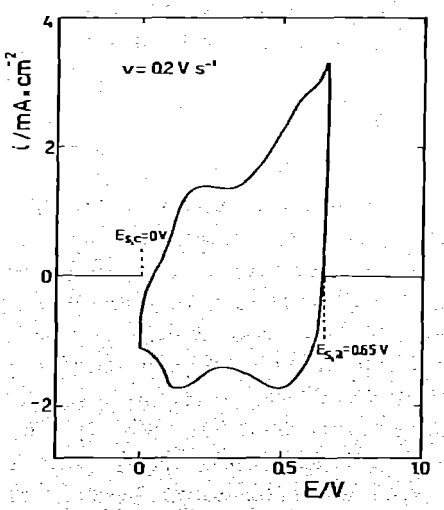

Fig. 5. Potentiodynamic RTPS E/I contour run at 0.2 V s^{-1}. Solution A.

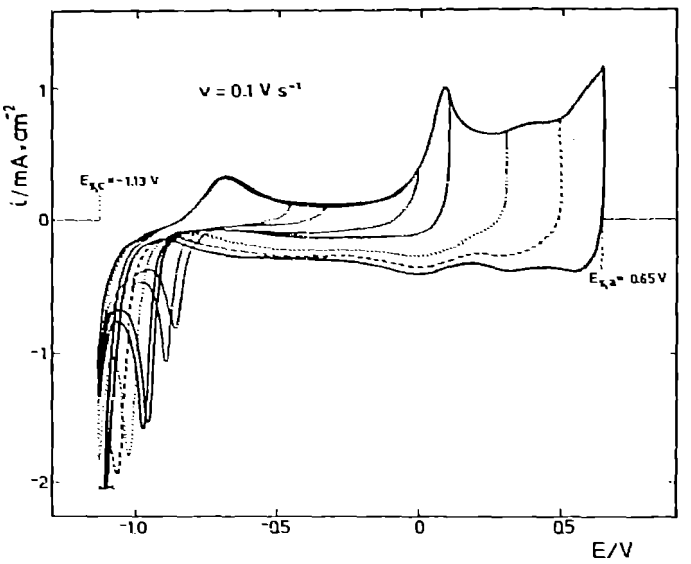

Fig. 6. Influence of the anodic switching potential on the cathodic E/I curves at 0.2 V s^{-1}. Solution B.

(Fig. 6). Thus, the electroreduction current peak which appears initially at −0.9 V, moves gradually towards more negative potentials as the anodic switching potential becomes more positive. Simultaneously, the electroreduction charge progressively increases. Furthermore, the hydrogen discharge reaction is then preceded by a small hump located at ca. −1.05 V. The changes of the E/I profile during the RTPS are independent of the stirring conditions of the electrolyte solution. The reversible characteristics of the three redox couples can be depicted through the TMTPS runs made at different amplitudes (ΔE_m) and sweep rate (υ_m) of the modulating signal (Figs. 7 and 8).

Vitreous carbon/$Co(OH)_2$/alkaline solution system

The preparation of colloidal $Co(OH)_2$ electrodes on vitreous carbon offers the possibility of obtaining data free from the possible electrodissolution of the base metal. As is already known for other colloidal hydroxide electrodes, when relatively thin Co hydroxide films are used, the electrochemical response of the system depends on the type of pretreatment applied to the base conducting material. Despite this, the potentiodynamic E/I profiles obtained with $Co(OH)_2$ precipitated on vitreous carbon previously immersed for 15 min in 1 : 1 $HNO_3 + H_2SO_4$ mixture, are, in principle, more poorly defined than those already described (Fig. 9). The voltammogram shows a charge decrease during the RTPS, the various redox systems are not well distinguished and probably—except for the redox couple located at more positive potentials—the rest of them are apparently kinetically slower than was

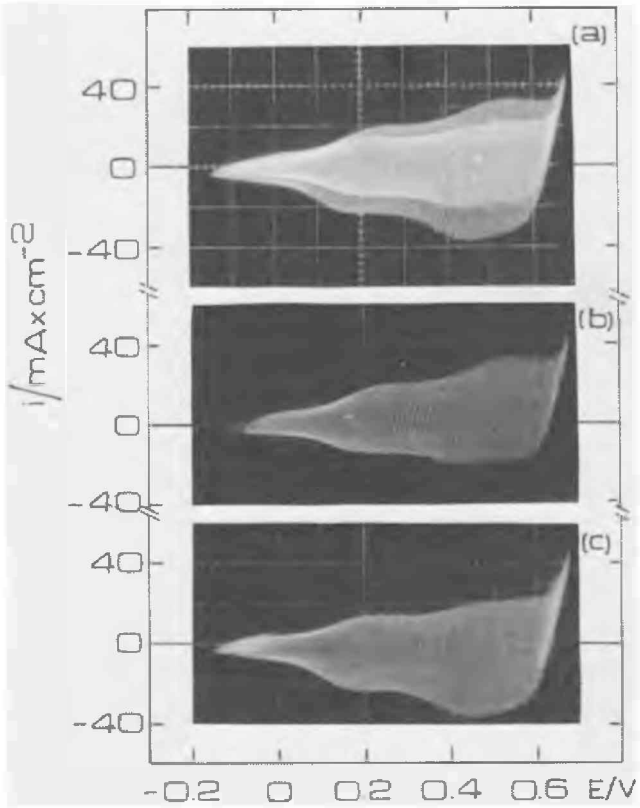

Fig. 7. (a) TMTPS voltammograms run between −0.15 and 0.66 V using $v_b = 0.5$ V s^{-1}, $v_m = 5$ V s^{-1} and $\Delta E_m = 0.045$ V; (b) positive-potential-going E/I contour corresponding to the display (a); (c) negative-potential-going E/I contour corresponding to the display (a). Solution E.

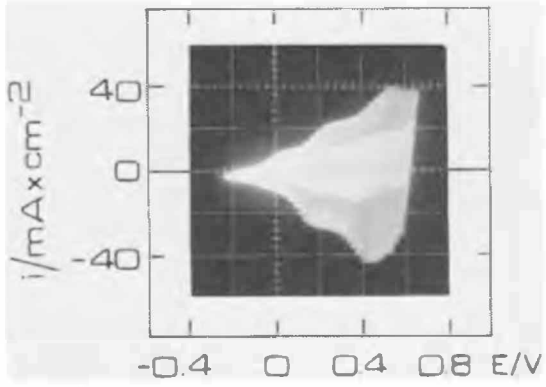

Fig. 8. E/I profile run with TMTPS using $v_b = 1$ V s^{-1}, $v_m = 6$ V s^{-1} and $\Delta E_m = 0.06$ V. Solution E.

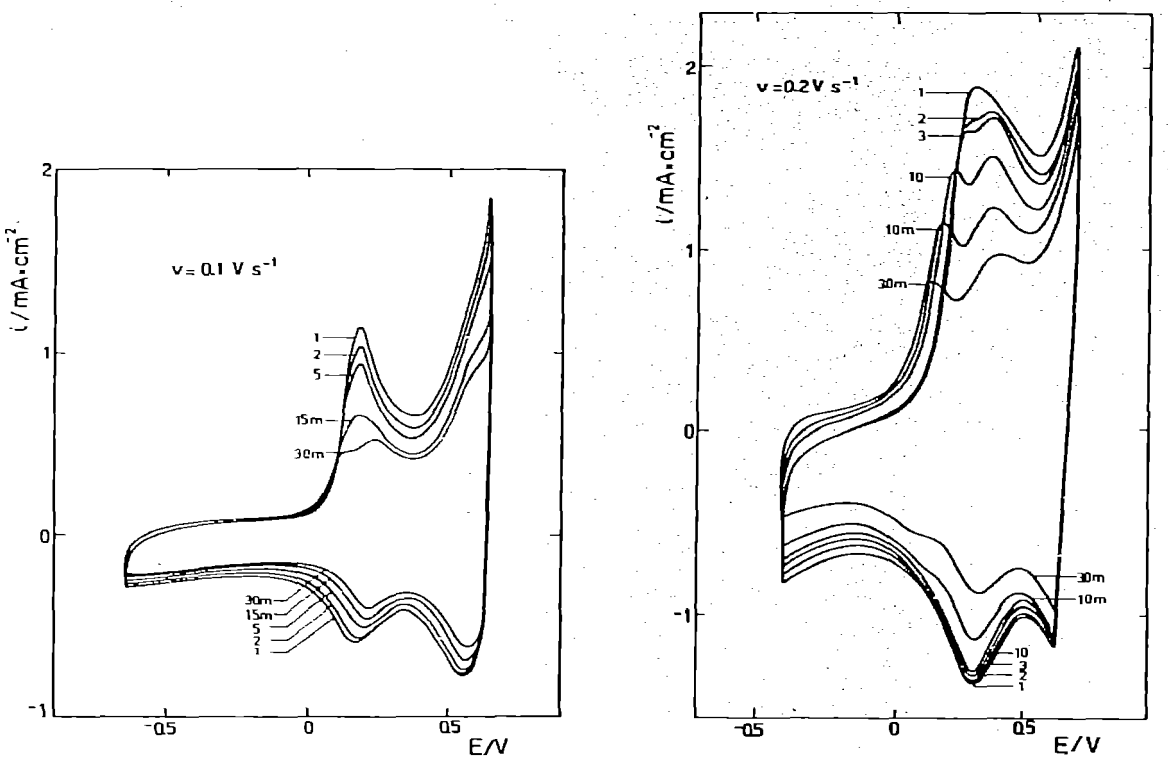

Fig. 9. Potentiodynamic RTPS E/I displays obtained with the vitreous-C/$Co(OH)_2$ electrode at 0.1 V s^{-1}. The cobalt hydroxide electrode was prepared by 10 alternative 10 s immersions in the precipitation solutions. Solution D.

Fig. 10. Potentiodynamic RTPS E/I displays obtained with the vitreous-C/$Co(OH)_2$ electrode at 0.2 V s^{-1}. The cobalt hydroxide electrode was prepared by 10 alternative 10 s immersions in the precipitation solutions. Solution D.

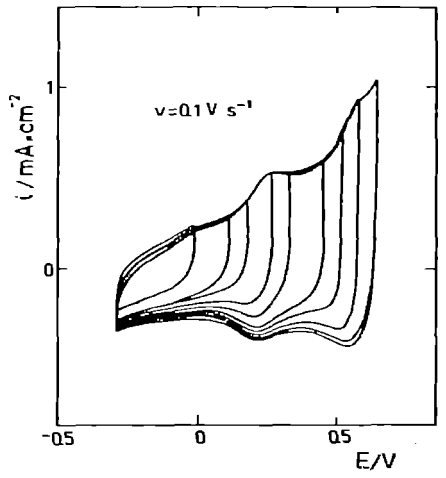

Fig. 11. Influence of the anodic switching potential on the cathodic E/I curves performed with the vitreous-C/$Co(OH)_2$ electrode at 0.1 V s^{-1}. Solution D.

earlier found on the cobalt base electrode. It should be noted that the definition of the three redox couples depends on the switching potential values (Fig. 10). The same conclusions are derived by running potentiodynamic E/I displays with a gradual increase of the anodic switching potential (Fig. 11). The charge related to the electro-oxidation of precipitated $Co(OH)_2$ increases with the number of alternative immersions in the precipitating solutions and decreases as the immersion time in those solutions increases. When the potential limit exceeds the oxygen evolution threshold, the negative-potential-going scan shows the electroreduction of molecular oxygen in the −0.6 to 0 V range. When this occurs, the immediately following positive-potential-going scan exhibits a small anodic current at ca. 0.1 V which is probably related to the electro-oxidation of a peroxidic-type intermediate produced during the preceding oxygen electroreduction [43–45].

DISCUSSION

The reversible characteristics of the electrochemical reactions occurring in the potential range between −0.5 and 0.65 V offer the possibility of a straightforward comparison of the potentials of the corresponding current peaks with those predicted by thermodynamics [6]. It is clear that the reactions in the lower potential range should be mainly related to Co(II)/Co(III) redox systems, while at potentials preceding the discharge of oxygen, the Co(III)/Co(IV) couple should predominate. According to Table 1, the potentials of all possible reactions should depend on the OH^- ion concentration in solution; however, this influence in the present case is, in principle, compensated because of the reference electrode used in the measurements.

Previous results on the behaviour of Co/alkaline solution interphases have shown the formation of a sandwich-type structure when the electrode was subjected to a prolonged potential cycling, namely a structure such as $Co/CoO/Co(OH)_2$ was proposed [42]. This sandwich-type structure has already been proposed by Sato [19],

TABLE 1

Standard equilibrium potentials in the Co/KOH system [6]

Conjugated redox couple	E/V (vs. Hg/HgO)
$Co_3O_4 + H_2O + 2e \rightleftharpoons 3\,CoO + 2\,OH^-$	−0.369
$Co_3O_4 + 4\,H_2O + 2e \rightleftharpoons 3\,Co(OH)_2 + 2\,OH^-$	−0.192
$CoOOH + e \rightleftharpoons CoO + OH^-$	−0.172
$CoOOH + H_2O + e \rightleftharpoons Co(OH)_2 + OH^-$	−0.054
$CoO_2 + H_2O + 2e \rightleftharpoons CoO + 2\,OH^-$	+0.195
$3\,CoOOH + e \rightleftharpoons Co_3O_4 + OH^- + H_2O$	+0.222
$CoO_2 + 2\,H_2O + 2e \rightleftharpoons Co(OH)_2 + 2\,OH^-$	+0.254
$3\,CoO_2 + 2\,H_2O + 4e \rightleftharpoons Co_3O_4 + 4\,OH^-$	+0.477
$CoO_2 + H_2O + e \rightleftharpoons CoOOH + OH^-$	+0.562

although it should be admitted, in principle, that for the same oxidation state, the degree of hydration of the two layers should depend on the conditions in which the complex electrochemical interphase has been formed, including the influence of the composition of the electrolyte solution. Therefore, when the electro-oxidation of cobalt in the alkaline electrolyte proceeds at potentials more positive than −0.5 V, then the reaction involves the oxidation of one of the two main Co(II) species which constitute the sandwich-type structure, namely, CoO and $Co(OH)_2$.

One interesting point to emphasize is the fact that all the voltammograms exhibit poorly distinguished current peaks which are mounted on a base line which are initiated at about −0.4 V in the anodic direction. The same applies in the negative-potential-going directions. Furthermore, along the whole potential range (−0.5–0.6 V) the electrochemical reactions behave as reversible processes similar to those encountered for other proton transfer reactions in transition metal hydroxide/oxyhydroxide systems [46–49]. From thermodynamic data it is concluded that the inner CoO layer is oxidized to Co_3O_4 according to

$$3\,(CoO)_{inner} + H_2O = Co_3O_4 + 2\,H^+ + 2\,e \qquad (1)$$

since the E^0 value for reaction (1) [E^0/(V, Hg/HgO) = −0.396 V] coincides with the potential where the Co(II) to Co(III) electrooxidation is initiated. The potential of reaction (1) is given by

$$E = -0.369 - (RT/2F)\,\ln\left(a^3_{CoO}/a_{Co_3O_4}\right) - (RT/F)\,\ln a_{OH^-} \qquad (2)$$

where the activities (a) of the two oxides refer to the conditions at the inner layer, which may, in principle be different from those in the bulk systems. According to eqn. (2) as the $a^3_{CoO}/a_{Co_3O_4}$ ratio decreases, the potential shifts in the positive direction and finally the electro-oxidation of the outer $Co(OH)_2$ layer becomes feasible. This means that within a certain range of potential a complex interface of the type $Co/CoO/Co_3O_4$ is also formed. This type of structure was actually found, under certain conditions, at the Co/alkaline solution interface [13].

According to the previous picture, the reversible characteristics of the reactions and the fairly good coincidence between the potentials of the conjugated current peaks with the thermodynamic data, the first process can be written as follows:

$$[Co(CoO)(Co(OH))_2 \cdot x\,H_2O] \rightarrow [Co(CoO)(CoOOH \cdot x'H_2O)] + H^+ + x''\,H_2O + e \qquad (3)$$

where $x' + x'' = x$. Accordingly, a second sandwich-type structure is formed in the first stage of the Co(II) to Co(III) electro-oxidation process. The current peak found at ca. 0.0 V, is close to the thermodynamic value corresponding to reaction (3), which is −0.054 V (Table 1). According to thermodynamics one would expect that the inner CoO layer is first electro-oxidized to Co(III), as the corresponding E^0 value is more negative than that of reaction (3). However, the sandwich-type structure implies that the OH^- ion concentration at the inner layer, as well as the water content, are determined to a great extent by the characteristics of the outer

$Co(OH)_2$. In this case, the equilibrium potential of the CoO/Co_3O_4 couple would be shifted towards more positive values. Therefore, after reaction (3) is completed, the electro-oxidation of CoO to Co_3O_4 is also finished. Afterwards the sandwich-type structure should approach the structure $Co/Co_3O_4/CoOOH$. Then, the following oxidation stage is the electro-oxidation of Co_3O_4 to CoOOH, according to the reaction

$$[Co(Co_3O_4 \cdot CoOOH)] + 2\,H_2O = [Co(CoOOH)_4] + H^+ + e \quad (4)$$

The E^0 value for reaction (4) coincides with the potential values of the second group of conjugated current peaks. It is likely that the inner layer is then not completely transformed into the oxyhydroxide species, because one should expect less activity of water at the inner-layer region. Finally, in the region preceding the O_2-evolution the electrochemical reaction yielding Co(IV) from Co(III) species should occur at a potential which, according to the following reactions:

$$Co_3O_4 + 4\,OH^- = 3\,CoO_2 + 2\,H_2O + 4\,e \quad (5)$$

and

$$CoOOH \rightarrow CoO_2 + H^+ + e \quad (6)$$

is close to 0.5 V, just in the range where the current peaks related to the third stage of the electro-oxidation process are observed.

In conjunction with the interpretation advanced above, the results obtained using conducting substrates other than cobalt can be understood, especially those referring to the changes produced during potentential cycling (Fig. 10). Thus, for the runs depicted in Figs. 9 and 10 the electrochemical system initially corresponds to the carbon/$Co(OH)_2$ interphase. Hence, the electro-oxidation reaction should exhibit peaks III and IV as the main contributions, as it actually occurs. But as the potential cycling covers the -0.5 V range, then part of the CoOOH is electroreduced to Co, and consequently the E/I profile gradually changes from the initial one to that resulting when cobalt itself was used as the base electrode material. These changes are also associated with the modification of the charges playing a part in the overall process under potentiodynamic conditions.

In any case, the behaviour of the processes discussed above indicates that the electrochemical reactions involve fast proton transfers and that the advance in the degree of oxidation of the metal is accompanied by a deprotonation and change in the water content at different parts of the complex electrochemical interface, in agreement with the general reaction pathway recently proposed to explain the active dissolution, active–passive transition and passivation of iron family metals in aqueous electrolytes [50–55]. This fact opens up the possibility that different $Co(OH)_2$ and CoOOH structures participate in the reactions occurring at slightly different potential regions, as is the case of nickel hydroxide electrodes. On fact, α- and β-$Co(OH)_2$ crystalline structures are reported in the literature [35]. It is reported that α-$Co(OH)_2$ electrodeposited on platinum electro-oxidizes in KOH solution to $CoO_{1.65}$ with a 5% content of potassium, yielding a crystalline structure which is

similar to that of γ-NiOOH. On the other hand, β-$Co(OH)_2$, having a brucite-type structure is very resistant to its electro-oxidation [4,29]. However, their electrochemical reactions are not so evident as in the case of nickel hydroxide electrode because the different electro-oxidation stages of cobalt from Co(II) to Co(IV) appear in a potential range which is smaller than that of nickel. The same applies to the existence of two CoOOH species, namely α- and β-CoOOH [29]. In this case, ageing effects such as those already described for the nickel hydroxide electrode are not discarded for the cobalt hydroxide electrode. At present, however, the complexity of the electrochemical reactions impedes a definite conclusion on this aspect of the reaction.

ACKNOWLEDGEMENTS

INIFTA is sponsored by the Consejo Nacional de Investigaciones Cientificas y Técnicas, the Universidad Nacional de La Plata and the Comisiôn de Investigaciones Cientificas (Provincia de Buenos Aires). This work was partially supported by the Regional Program for the Scientific and Technological Development of the Organization of American States. H.G.M. is grateful to the Universidad Católica de Valparaiso for the award of a research fellowship.

REFERENCES

1 G. Grube and O. Feucht, Z. Elektrochem., 28 (1922) 568.
2 G. Grube, Z. Elektrochem., 33 (1927) 398.
3 S.E.S. El Wakkad and A. Hickling, Trans. Faraday Soc., 46 (1950) 820.
4 P. Benson, G.W.D. Briggs and W.F.K. Wynne-Jones, Electrochim. Acta, 9 (1964) 281.
5 R.D. Cowling and A.C. Riddiford, Electrochim. Acta, 14 (1969) 981.
6 W.K. Behl and J.E. Toni, J. Electroanal. Chem., 31 (1971) 63.
7 T.R. Jayaraman, V.K. Venkatesan and H.V.K. Udupa, Electrochim. Acta, 20 (1975) 209.
8 V.V. Klepikov, V.V. Sysoeva and N.N. Milyutin, Zh. Prikl. Khim., 50 (1977) 2256.
9 A. Déchenaud, C. Guillet, I. Barralis and J. Lédion, Métaux, 631 (1978) 71.
10 R.V. Boldin, Elektrokhimiya, 3 (1967) 1259.
11 V.V. Klepikov, V.V. Sysoeva and R.V. Boldin, Zh. Prikl. Khim., 51 (1978) 1904.
12 V.T. Solodun, D.A. Baitalov and F.F. Faizullin, Zashch. Met., 16 (1980) 315.
13 L.D. Burke and O.J. Murphy, J. Electroanal. Chem., 109 (1980) 373.
14 L.D. Burke and O.J. Murphy, J. Electroanal. Chem., 112 (1980) 379.
15 T. Ohtsuka and N. Sato, J. Jap. Inst. Met., 39 (1975) 60.
16 T. Ohtsuka and N. Sato, Boshoku Gijutsu, 24 (1975) 289.
17 T. Ohtsuka, K. Kudo and N. Sato, J. Jap. Inst. Met., 40 (1976) 124.
18 K. Kudo, N. Sato and T. Ohtsuka in R.P. Frankenthal and J. Kruger (Eds.), Passivity of Metals, The Electrochemical Society, Princeton, 1978 p. 918.
19 N. Sato and T. Ohtsuka, J. Electrochem. Soc., 125 (1978) 1735.
20 D.H. Davies and G.T. Burstein, Corros. Sci., 20 (1980) 973.
21 G.T. Burstein and D.H. Davies, Corros. Sci., 20 (1980) 989.
22 W. Paik and J.O'M. Bockris, Surf. Sci., 28 (1971) 61.
23 G.W. Simmons, A. Vértes, M.L. Varsányi and H. Leidheiser, J. Electrochem. Soc., 126 (1979) 187.
24 G.W. Simmons, E. Kellerman and H. Leidheiser, J. Electrochem. Soc., 123 (1976) 1276.
25 G.W. Simmons in R.P. Frankenthal and J. Kruger (Eds.), Passivity of Metals, The Electrochemical Society, Princeton, 1978, p. 898.

26 G.W. Simmons and H. Leidheiser, Mössbauer Eff. Methodol., 10 (1976) 215.
27 W.M. Latimer, Oxidation Potentials. The Oxidation States of the Elements and Their Potentials in Aqueous Solutions, 2nd edn., Prentice-Hall, New York, 1952.
28 A.J. de Bethune and N.A. Swendeman Loud, Standard Aqueous Electrode Potentials and Temperatures Coefficients at 25°C, Hampel, Skokie, Ill., 1964.
29 P. Benson, G.W.D. Briggs and W.F.K. Wynne-Jones, Electrochim. Acta, 9 (1964) 275.
30 M. Pourbaix, Atlas of Electrochemical Equilibria in Aqueous Solutions, Pergamon, New York, 1966.
31 H. Göhr, Electrochim. Acta, 11 (1966) 827.
32 H. Bode, K. Dehmelt and J. Witte, Electrochim. Acta, 11 (1966) 1079.
33 R.N. Goldberg, R.G. Riddell, M.R. Wingard, H.P. Hopkins, C.A. Wulff and L.G. Hepler, J. Phys. Chem., 70 (1966) 706.
34 J.W. Larson, P. Cerutti, H.K. Garber and L.G. Hepler, J. Phys. Chem., 72 (1968) 2902.
35 G.W.D. Briggs, Specialist Periodical Reports on Electrochemistry, Vol. 4, The Chemical Society, London, 1974, p. 43.
36 V.V. Shalagonov, I.D. Belova, Yu.E. Roginskaya and D.M. Shub, Elektrokhimiya, 14 (1978) 1708.
37 G.I. Zakharkin, M.R. Tarasevich and A.M. Khulornoi, Zh. Fiz. Khim., 51 (1977) 3068.
38 B.N. Efremov, S.R. Zhukov, G.I. Zakharkin and M.R. Tarasevich, Elektrokhimiya, 14 (1978) 936.
39 B.N. Efremov, M.R. Tarasevich, G.I. Zakharin and S.R. Zhukov, Elektrokhimiya, 14 (1978) 1504.
40 B.N. Efremov, G.I. Zakharin, M.R. Tarasevich and S.R. Zhukov, Zh. Fiz. Khim., 52 (1978) 1671.
41 V.V. Klepikov and V.V. Sysoeva, Zh. Prikl. Khim., 51 (1978) 2396.
42 H. Gomez Meier, J.R. Vilche and A.J. Arvia, J. Electroanal. Chem., 134 (1982) 251.
43 J.V. Butler and G. Drever, Trans. Faraday Soc., 32 (1936) 427.
44 M.O. Davies, M. Clark, E. Yeager and F. Hovovka, J. Electrochem. Soc., 106 (1959) 56.
45 L.N. Chetyrbok, V.I. Naumor, G.F. Volodin and Yu.M. Tyurin, Elektrokhimiya, 14 (1978) 1750.
46 R.S. Schrebler Guzmán, J.R. Vilche and A.J. Arvia, J. Electrochem. Soc., 125 (1978) 1578.
47 M.E. Folquer, J.R. Vilche and A.J. Arvia, J. Electrochem. Soc., 127 (1980) 2634.
48 V.A. Macagno, J.R. Vilche and A.J. Arvia, J. Appl. Electrochem., 11 (1981) 417.
49 J.O. Zerbino, J.R. Vilche and A.J. Arvia, J. Appl. Electrochem., 11 (1981) 703.
50 R.S. Schrebler Guzmán, J.R. Vilche and A.J. Arvia, J. Appl. Electrochem., 9 (1979) 321.
51 S.G. Real, J.R. Vilche and A.J. Arvia, Corros. Sci., 20 (1980) 563.
52 H. Gomez Meier, J.R. Vilche and A.J. Arvia, J. Appl. Electrochem., 10 (1980) 611.
53 J.R. Vilche and A.J. Arvia, Acta Cient. Venez., 31 (1980) 408.
54 J.R. Vilche and A.J. Arvia, Anal. Acad. Cs. Ex. Fis. Nat. Arg., 33 (1981) 33.
55 M. Lopez Teijelo, J.R. Vilche and A.J. Arvia, J. Electroanal. Chem., 131 (1982) 331.